Fracture strength of the proximal femur injected with a calcium sulfate/hydroxyapatite bone substitute

Kok, Joeri; Širka, Aurimas; Grassi, Lorenzo; Raina, Deepak Bushan; Tarasevičius, Šarūnas; Tägil, Magnus; Lidgren, Lars; Isaksson, Hanna

Published in:
Clinical Biomechanics

DOI:
10.1016/j.clinbiomech.2019.03.008

2019

Document Version:
Publisher's PDF, also known as Version of record

Clinical Biomechanics 63 (2019) 172–178

Contents lists available at ScienceDirect

Clinical Biomechanics

journal homepage: www.elsevier.com/locate/clinbiomech

Fracture strength of the proximal femur injected with a calcium sulfate/hydroxyapatite bone substitute

Joeri Kok[a,*], Aurimas Širka[b], Lorenzo Grassi[a], Deepak Bushan Raina[c], Šarūnas Tarasevičius[b], Magnus Tägil[c], Lars Lidgren[c], Hanna Isaksson[a,c]

[a] Department of Biomedical Engineering, Lund University, Box 118, 221 00 Lund, Sweden
[b] Department of Orthopedics and Traumatology, Lithuanian University of Health Sciences, A. Mickevičiaus g. 9, LT 44307 Kaunas, Lithuania
[c] Department of Orthopedics, Clinical Sciences, Lund University, Box 118, 221 00 Lund, Sweden

ARTICLE INFO

Keywords:
Prophylactic injection
Ceramics
Hip fracture
Finite element analysis
Bone strength
Osteoporosis

ABSTRACT

Background: Available interventions for preventing fragility hip fractures show limited efficacy. Injection of a biomaterial as bone substitute could increase the fracture strength of the hip. This study aimed to show the feasibility of injecting a calcium sulfate/hydroxyapatite based biomaterial in the femoral neck and to calculate the consequent change in strength using the finite element method.
Methods: Five patients were injected with 10 ml calcium sulfate/hydroxyapatite in their femoral neck. Quantitative CT scans were taken before and after injection. Five additional patients with fragility hip fractures were also scanned and the images from the non-fractured contralateral sides were used. Finite element models were created for all proximal femora with and without injection and the models were tested under stance and sideways fall loading until fracture. The change in fracture strength caused by the injection was calculated. Additionally, perturbations in volume, location, and stiffness of the injected material were created to investigate their contribution to the fracture strength increase.
Findings: The 10 ml injection succeeded in all patients. Baseline simulations showed theoretical fracture strength increases of 0–9%. Volume increase, change in location and increase in stiffness of the material led to increases in fracture strength of 1–27%, −8-26% and 0–17%, respectively. Altering the location of the injection to a more lateral position and increasing the stiffness of the material led to increases in fracture strength of up to 42%.
Interpretation: This study shows that an injection of calcium sulfate/hydroxyapatite is feasible and can theoretically increase the hip's fracture strength.

1. Introduction

The socio-economic burden of osteoporosis is substantial and besides patient morbidity, costs associated with management of osteoporotic fractures have been estimated to be close to €100 billion in Europe (Hernlund et al., 2013). A statistical model analyzing the increase in osteoporosis related fractures in the U.S and their costs between 2005 and 2025 indicates that the annual fracture rate and associated costs will increase by 50% (Burge et al., 2007). One of the most common anatomical locations for fragility fractures is the hip and more specifically the femoral neck (Warriner et al., 2011). Patients that have already suffered from a first hip fracture have particularly high risk of a second hip fracture (Sobolev et al., 2015). In the Framingham Heart Study, 15% of subjects experienced a second hip fracture during a median of 4.2 years of follow-up (Berry et al., 2008). In this same study the one-year mortality following a second hip fracture was 24%, while the one-year mortality following an initial hip fracture was 16%. Thus, there is a clinical need for prevention of fragility hip fractures both from a patient and a socio-economic perspective.

Patients with an increased fracture risk are generally treated with pharmacological interventions, such as bisphosphonates. However, their effectiveness in terms of preventing hip fractures is limited (Järvinen et al., 2015), partially due to a delayed response to the treatment of 9–16 months (Ferrari et al., 2016). This delay in response is especially problematic for patients at very high risk of secondary fracture and high mortality risk. Furthermore, systemic bisphosphonates may induce atypical cortical fractures by suppressing the physiological bone remodeling cycles caused by the apoptotic effect of

* Corresponding author at: Department of Biomedical Engineering, BMC - D13, 221 84 Lund, Sweden.
E-mail addresses: joeri.kok@bme.lth.se (J. Kok), lorenzo.grassi@bme.lth.se (L. Grassi), deepak.raina@med.lu.se (D.B. Raina), magnus.tagil@med.lu.se (M. Tägil), hanna.isaksson@bme.lth.se (H. Isaksson).

https://doi.org/10.1016/j.clinbiomech.2019.03.008
Received 10 January 2019; Accepted 11 March 2019

bisphosphonates on osteoclasts (Saita et al., 2015). External hip protectors have potential for reducing the impact of a fall on the femur, but suffer from low patient compliance (Santesso et al., 2014).

A more recent development in prophylactic approaches is femoroplasty, where the femoral neck is augmented by injecting a material, most commonly polymethyl methacrylate (PMMA). One of the first ex-vivo experimental studies in the proximal femur injected 28–41 ml of PMMA. The peak force increased with 21% in single leg stance and 82% in sideways fall loading (Heini et al., 2004). Later, both ex-vivo experimental and computational studies aimed to optimize the injection volume and location. Experimentally, this resulted in strength increases up to 30–35% with 10–12 ml injections (Basafa et al., 2015; Beckmann et al., 2011). In-silico computational studies using finite element (FE) simulations showed an increase in fracture strength up to 59% with a 12 ml injection (Varga et al., 2017). All together, these studies show a great potential of the technique. However, they all used PMMA, and the protocols were either not tested for clinical feasibility or required complex patient-specific planning and robotic injection devices. Besides this, the risk of damaging surrounding tissue and the ethical concerns surrounding invasive treatment of non-fractured bone remain, leading to low clinical acceptance (Varga et al., 2016).

As an alternative to PMMA, apatite-based biomaterials like injectable biphasic calcium sulfate/hydroxyapatite (CaS/HA) could be used for femoroplasty. Several variations of this material are approved for clinical applications (Nilsson et al., 2013) and CaS/HA has previously been suggested as an alternative for PMMA in e.g. vertebral compression fractures (Masala et al., 2012). However, the clinical feasibility of injecting CaS/HA in the hip and its potential to increase the fracture strength has not been studied.

In this study we first aimed to show that an injection of CaS/HA into the femoral neck is feasible. Secondly, a computational study using the FE method was performed to calculate the resulting increase in bone fracture strength after an injection. Finally, we aimed to determine how variations in injected volume, location and stiffness of the injected material can affect the increase in fracture strength as a base for local prevention in patients at high risk for fragility hip fractures.

2. Methods

2.1. Patients and imaging

2.1.1. THR group

Five patients coming in for total hip replacement (THR) surgery were first imaged using quantitative computed tomography (QCT) (Lightspeed Pro 16, GE, Chicago, USA) (120 kVp, 647–697 mA, 2.5 mm slice spacing, 0.7–1.0 mm in-plane voxel size) (Fig. 1A) using a bone density calibration phantom (QRM-BDC/6, Quality Assurance in Radiology and Medicine, Moehrendorf, Germany). Before surgery, the hip was prepared in a sterile manner and dressed using sterile single-use adhesive drapes. A 12 cm bone biopsy needle with cannula (13 G) was percutaneously introduced through the lateral cortex of the proximal femoral shaft at the level of the upper part of the lesser trochanter. The cannula position in the femoral neck and material spreading during the injection was controlled and monitored with fluoroscopy (Arcadis Orbic mobile C-arm, Siemens, Erlangen, Germany) (23 mA, 2.3 Kw generator power, 0.6 mm maximum focal spot) using standardized AP and lateral views of the proximal femur (Fig. 1B). All patients received an injection of 10 ml CaS/HA (Cerament™ Bone Void Filler, Bone Support AB, Lund, Sweden). The material was mixed using a standardized technique and injected using passive retraction with the tip of the needle slowly being retracted through the cervical neck into the trochanter. After material injection all patients were placed in a lateral position and the total hip replacement surgery using posterolateral approach was performed. After femoral neck osteotomy all femoral heads were excised and imaged using QCT (Lightspeed Pro 16, GE, Chicago, USA) (120 kVp, 198 mA, 2.5 mm slice spacing, 0.5 mm in-plane voxel size) (Fig. 1C).

2.1.2. Hip fracture group

A second group of five patients with fragility hip fractures was included in the study. These patients were not injected with the biphasic material. They represented an osteoporotic cohort and were only used for the FE-modeling part of the study. They had their contralateral, non-fractured, hips imaged using QCT (Lightspeed Pro 16, GE, Chicago, USA) (120 kVp, 647–697 mA, 2.5 mm slice spacing, 0.5–0.9 mm in-plane voxel size) using the same calibration phantom as the THR group. DXA scans were taken (Discovery Ci, Hologic, Marlborough, USA) to confirm that all these patients were osteoporotic (Table 1).

All human experiments were approved by the Kaunas Regional Committee of Ethics of Biomedical Researches (ethical permission number: BE-2-40, 2017-06-26).

2.2. Image processing and finite element models

For the THR group, proximal femora of all patients were segmented from the QCT images before surgery (Seg3D2, University of Utah, Salt Lake City, USA). The QCT images of the excised femoral heads were used to segment the injected material and the femoral head. These segmentations were processed to obtain a surface geometry (Autodesk Meshmixer 3.4.35, Autodesk, San Rafael, USA). The geometry of the proximal femur and the femoral head, together with the biphasic material geometry, were aligned using an in-house registration algorithm based on the iterative closest point algorithm. None of the excised femoral heads contained the full injection, so the fluoroscopy images were used to estimate the location of the full injection and the biphasic material geometry was extended to cover a total volume of 10 ml. The surface geometries of the proximal femur and injection volume were transformed into a solid geometry (Solidworks 2016, Dassault Systèmes, Vélizy-Villacoublay, France). Using a Boolean equation, the region covered by the injection was removed from the femur geometry (HyperMesh 2017, Altair Engineering, Troy, USA). Second order tetrahedral elements were used to mesh both geometries (total of ~100 k elements and ~140 k nodes). Nodes within 0.1 mm from one another between the two meshes were set to be equivalent to create one final mesh without surface intersections.

For the hip fracture patients, who did not receive an injection, the geometry of the injected material from the patient with the highest

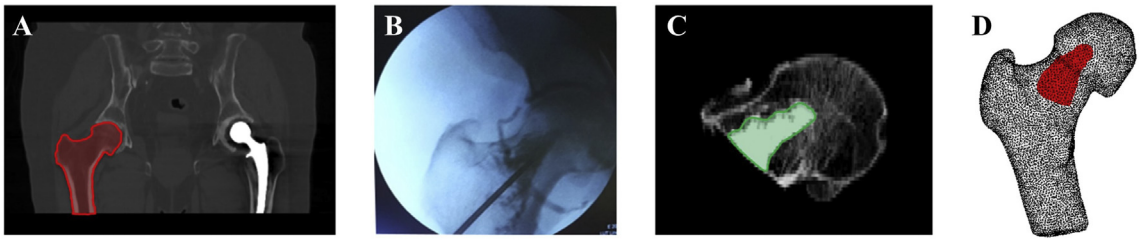

Fig. 1. (A) Preoperative CT-scan with bone segmentation. (B) Intraoperative fluoroscope image. (C) Postoperative CT-scan of the femoral head and neck with biphasic material segmentation. (D) Final FE mesh of the femur with 10 ml injected material.

Table 1
Patient morphometrics. Patients are numbered based on areal bone mineral density (aBMD) as calculated from QCT. This was done by projecting and normalizing the QCT obtained volumetric bone mineral densities [g/cm^3] in a region similar to DXA. Thus a higher patient number indicates a more severely osteoporotic patient. OA: osteoarthritis; ON: osteonecrosis; HF: hip fracture.

Patient	1	2	3	4	5	6	7	8	9	10
Sex	m	m	m	f	f	f	f	f	f	f
Clinical status	OA	OA	ON	OA	OA	HF	HF	HF	HF	HF
Age	73	71	54	75	68	88	77	85	83	94
Weight	86	82	74	75	69	50	79	60	72	75
Height	180	173	180	158	161	150	160	162	168	162
T-score	N/A	N/A	N/A	N/A	N/A	−3.5	−2.9	−2.7	−2.7	−3.5
aBMD DXA neck [g/cm^2]	N/A	N/A	N/A	N/A	N/A	0.458	0.531	0.551	0.552	0.456
aBMD QCT neck [g/cm^2]	1.023	0.963	0.952	0.824	0.817	0.546	0.543	0.514	0.507	0.437

injection volume in the excised femoral head was used. This geometry was manually inserted to fit in the femoral neck of the proximal femur geometries. It was ensured that a similar positioning of the material as in the THR patients was achieved. The rest of the modeling strategy was kept the same.

Bone was modeled as a heterogeneous isotropic linear elastic material with a Poisson's ratio of 0.4. The elastic modulus was obtained from calibrated CT values (Morgan et al., 2003; Schileo et al., 2014) using BoneMat_V2 (Taddei et al., 2007). The region considered to contain the injected material was modeled as bone with the exception that the stiffness of each element was increased by 500 MPa, which is the elastic modulus of the injected material, based on data provided by the manufacturer (Bone Support AB, Lund, Sweden). Additionally, all elements at the surface of the mesh were considered to be cortical bone and were assigned a minimum stiffness of 500 MPa. Two loading conditions were considered, single leg stance (SLS) and sideways fall (SWF) (Fig. 2).

2.3. Variations of the modeled injection

For each patient the baseline injection in the models was varied according to three schemes: changing the volume of the injection, altering the location of the injection, or changing the material properties of the injected material. In all cases the mesh was kept the same, and elements at the surface of the mesh were regarded as cortical bone and were not allowed to be penetrated by the injection.

2.3.1. Volume of the injection

The injected volume was increased by letting it grow in four different directions (Fig. 3).

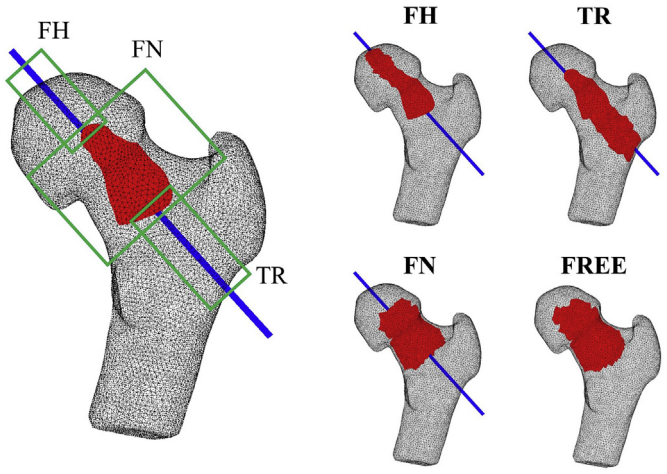

Fig. 3. Definition of the growth directions with use of a vector along the direction of injection. Each increment added one layer of elements connected to the baseline injection, by moving elements defined as bone to the region covered by the injection. First, growth was only allowed in the direction of the femoral head from elements at the tip of the baseline with new elements having at least one node within 5 mm of the vector (femoral head, FH). Second, growth was only allowed in the direction of the intertrochanteric region from the back of the baseline with new elements having at least one node within 8 mm of the vector (trochanter, TR). Third, growth was limited to the femoral neck by growing radially outwards from the injection line but not forwards or backwards (femoral neck, FN). Lastly, growth was left free in all directions (FREE).

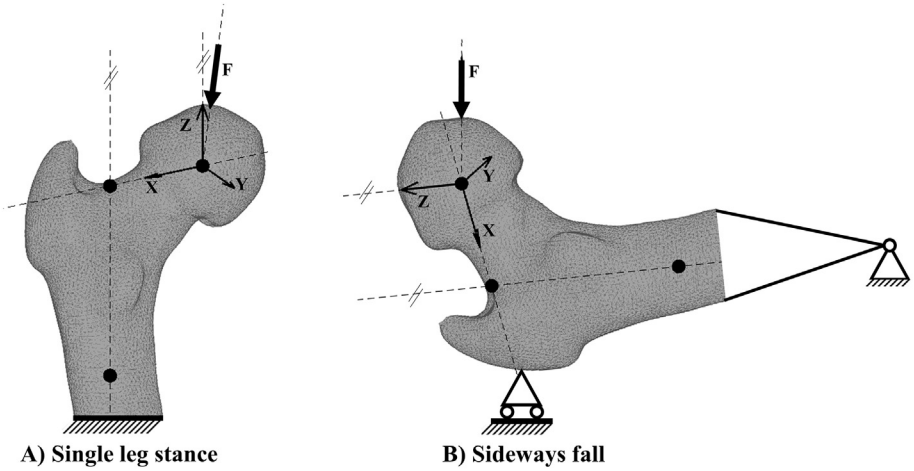

Fig. 2. The two loading conditions for each model. The loading conditions were set by first defining a reference frame in four steps. 1) The center of the femoral head was found by fitting a sphere around the femoral head and placed at the origin of the coordinate system. 2) An axis was defined between the centroid of the segmentation 20 mm below the minor trochanter and a manually placed landmark in the trochanteric fossa. 3) The whole geometry was rotated to fit this axis into the frontal plane parallel to the vertical axis of the coordinate system. All nodes on the surface of the mesh more than 50 mm below the minor trochanter were defined as base nodes. (A) For Single leg stance (SLS) the mesh was rotated to 8 degrees adduction from the reference frame and fixing the base nodes in all degrees of freedom and applying a load in the inferior direction on the 10 most superior nodes on the surface of the mesh. (B) For Sideways fall (SWF) the mesh was rotated to 10 degrees adduction and 15 degrees internal rotation and fixing the 50 most lateral nodes in the lateral-medial direction and applying a load in the lateral direction on the 10 most medial nodes on the femoral head.

Table 2
Calculated fracture strength [N] and relative fracture strength increase [%] of each patient before and after injection of biphasic material. Patients are ordered by aBMD as calculated from QCT. SLS: Single leg stance; SWF: Sideways fall.

Patient	1	2	3	4	5	6	7	8	9	10
SLS no injection	9313	14,891	9656	5587	8297	2579	3925	3075	4274	2327
SLS baseline injection	9468	15,001	9810	5717	8575	2682	3921	3301	4358	2421
	2%	1%	2%	2%	3%	4%	0%	7%	2%	4%
SWF no injection	3916	5005	4901	2980	1916	1039	1622	1626	1581	1596
SWF baseline injection	3996	5184	4945	3002	2014	1076	1690	1767	1621	1708
	2%	4%	1%	1%	5%	4%	4%	9%	3%	7%

2.3.2. Location of the injection

The volume was kept constant at 10 ml, and instead the location and shape of the injection was changed to seven different locations. These were: lateral (L), distal medial (DM), proximal medial (PrM), proximal lateral (PrL), intertrochanteric region (ITR), anterior lateral (AL), posterior lateral (PoL). In each femur, one element in each of seven locations was selected (Table 2). From each of the elements, the volume was grown in all directions using the same algorithm as in the previous section, until the injected volume reached 10 ml. When the last growth increment exceeded 10 ml, elements from the last increment with the highest density were removed, reducing the injected volume to 10 ml.

2.3.3. Stiffness of the injection

The effect of the injected material stiffness on the reinforcement of the femur was investigated by changing its elastic modulus value from the baseline level (+500 MPa) to +1000 MPa and +2000 MPa. This was simulated on all baseline injections as well as for varied injection locations.

2.4. Data analysis

All FE simulations were solved in Abaqus 2017 (Simulia, Dassault Systèmes, Vélizy-Villacoublay, France). Fracture strength of each model was calculated using a strain-based failure criterion that was earlier validated for linear elastic models of the proximal femur under SLS and SWF loading conditions (Schileo et al., 2014). In short, the maximum and minimum principal strains of the nodes on the surface are monitored and for each of these nodes the average strain in a 3 mm radius is calculated. The strains and applied load are then monitored until a strain of 0.73% in tension or 1.04% in compression is reached for one of the nodes (Bayraktar et al., 2004). The node that first fails is considered as the fracture location and the load required to reach this strain is the fracture strength. Because of possible artificially high strains close to the applied boundary conditions, all nodes within a 6-element distance of the boundary conditions are excluded from the determination of the fracture strength.

The fracture strength of each of the models with an injection was compared to the fracture strength of the corresponding femur without injection. For the models with the volume increase the calculated fracture strength at each increment was compared to the fracture strength of the baseline injection to quantify the further increase in fracture strength due to the increase in volume.

3. Results

Injection of 10 ml biphasic material was possible in all patients. The material was injected in the closed cavity using passive retraction with the tip of the needle slowly being retracted until the basis of the femoral neck. In one of the patients no spreading of the material was observed until the tip of the injection needle was retracted, leaving the injected material mostly in the intertrochanteric region. In one patient some material leakage into the lateral and medial circumflex arteries was observed.

FE simulations of the baseline injection resulted in a minor increase in fracture strength compared to the untreated cases (between 0 and 7% in SLS and 1–9% in SWF, Table 2). Generally, the patients with the highest relative increase in fracture strength were the osteoporotic patients within the lowest range of aBMD calculated from the QCT images.

For the variations of the modeled injection only the results for the fracture group in SWF are reported, because this has the highest clinical relevance. Additional results can be found in the supplementary data.

3.1. Volume of the injection

In most cases, an increase in the volume of the injected material led to an additional increase in fracture strength. This increase was, however, highly sensitive to the growth direction, as shown in Fig. 4 for the

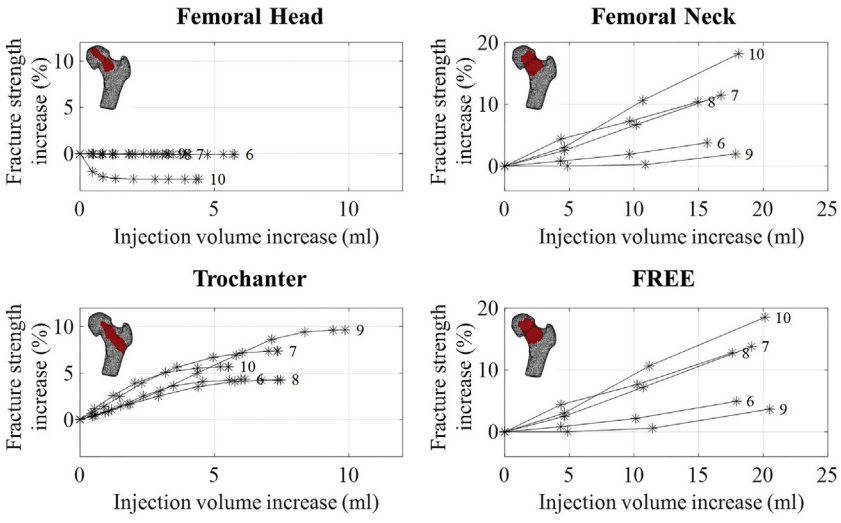

Fig. 4. Additional increase in fracture strength in response to incremental increase in injected volume for the five hip fracture patients in SWF. Numbers next to each line represent the individual patient ranking in aBMD (Table 1). Fracture strength increase was calculated by comparing the fracture strength of each model to the fracture strength of the same femur with the baseline injection.

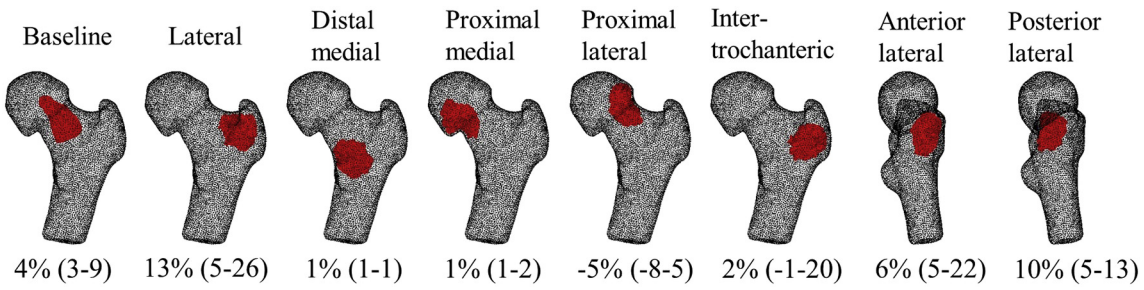

Fig. 5. All simulated variations of injection location with the fracture strength increase [%] presented as median (range) for the five hip fracture patients in SWF. Fracture strength increase was calculated by comparing the fracture strength of each model to the fracture strength of the same femur without injection.

hip fracture patients in SWF. Extending the injection further into the femoral head showed no positive effect on the femoral strength in SWF. At low volumes an increase of volume towards the intertrochanteric region had the highest effect of the tested volume increases, 0.7–2.1%/ml. Limiting the growth to the femoral neck and leaving the growth free generally resulted in a larger relative volume increase, 15–18 ml and 18–21 ml respectively, which subsequently also resulted in a higher increase in fracture strength, 2–18% and 4–19%, respectively.

3.2. Location of the injection

Keeping the injected volume fixed to 10 ml while varying the injection location resulted in high variation in fracture strength (Fig. 5). The location that showed the highest effect for 3 out of 5 fracture patients in SWF was the lateral region of the femoral neck (lateral). The other 2 fracture patients showed the highest increase in fracture strength with the injection in the posterior lateral location.

3.3. Stiffness of the injection

Simulations of injections of a material with a higher stiffness showed an increase in fracture strength (Fig. 6). A combination of a more optimal location and higher stiffness increase for the injection led to strength increases of 11–42%.

4. Discussion

In this study the feasibility to inject 10 ml of CaS/HA into the femoral neck has been investigated in vivo, and the resulting increase in fracture strength was calculated. Perturbations in injected volume, location and stiffness were tested using FE models to find out what could theoretically further increase the fracture strength.

CaS/HA was successfully injected into the femoral neck of all five patients. No prior debridement of the marrow/trabecular bone was performed to create larger space in cancellous bone and high pressure was required to inject the 10 ml of material in some patients. Patients in the THR group were operated due to advanced osteoarthrosis of the hip joint with dense subchondral bone. Thus, the challenges of injecting these patients were even higher since the patients were non-osteoporotic and had a relatively high bone density. In one patient radiolucency in the lateral and medial circumflex arteries was observed, indicating leakage of the material or radiographic contrast agent into the vessels. This may be explained by the controlled hypotension and decrease in arterial resistance to the pressure, a common procedure during spinal anesthesia. It could be speculated that it is not feasible to inject substantially larger volumes that would fill the femoral canal without damaging surrounding tissue and having material or contrast agent leakage into the circumflex arteries. Injections of slightly larger volumes may be feasible in patients with severe osteoporosis, but we concluded that 10 ml serves as a reasonable volume indicator for local femoral neck injections.

FE simulations with and without injection showed a large variation in predicted fracture forces both between the two patient groups and between individual patients in each group (Table 2). This implies that, regardless of clinical status, the viability of the treatment for the individual patients is difficult to predict. For all patients, the predicted increase in fracture strength was rather limited for both loading conditions (up to 9%). This suggested that the volume was insufficient, the location was not optimal, and/or the material properties of the injected material were not sufficient. Therefore, we continued investigating these parameters to find out which of these options can, theoretically, further increase the fracture strength.

When varying the volume of the injection, we found that the calculated increase in femoral strength was highly dependent on the direction of the volume increase. The highest initial increase in fracture strength per unit volume occurred when extending the volume towards the intertrochanteric region. For the fracture patients, no further increase in fracture strength was seen when extending the volume into the femoral head.

Altering the injection locations, the highest increases in fracture strength were achieved with the injection in the lateral and posterior lateral locations. These results agree with previous studies that investigated the optimal location for strength increase in SWF. Basafa et al. indicated the superior and inferior parts of the femoral neck and supero-posterior aspect of the greater trochanter (Basafa et al., 2015; Basafa and Armand, 2014) and Beckmann et al. the single centrodorsal (Beckmann et al., 2011) location as most efficient in increasing fracture strength.

Increasing the stiffness of the injected material in the models led to a further increase in fracture strength. This stiffening of the material gives a closer comparison to the stiffness expected when injecting PMMA (2140 MPa) (Kinzl et al., 2011). When increasing the stiffness

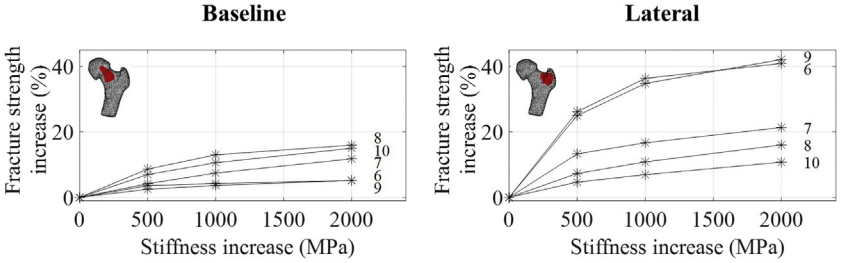

Fig. 6. The fracture strength increase for various stiffness increases of the injected material for the five hip fracture patients in SWF. Data is based on 10 ml injections in the locations covered by the baseline and lateral injection site. Numbers next to each line represent the individual patient ranking in aBMD (Table 1). Fracture strength increase was calculated by comparing the fracture strength of each model to the fracture strength of the same femur without injection.

with the injection in different locations an additional increase in fracture strength was observed, in some patients more than 40%. Other computational studies showing higher strength increases use optimization strategies (Basafa et al., 2015; Varga et al., 2017), which were not used in this study to keep the applied strategy clinically transferable.

An important, remaining, unanswered question is what level of strength increase is clinically relevant. One way to look at the required strength increase for each individual patient is to calculate the load-to-strength ratio, in which the strength of the femur is directly compared to the load on the femur experienced during a sideways fall. Keaveny and Bouxsein presented a cohort where ~6% of patients would theoretically be helped with an increase in fracture strength of only 5% (Keaveny and Bouxsein, 2008). A prospective case-cohort study by Orwoll et al. calculated an average load-to-strength ratio for fracture cases of 1.13 suggesting that, on average, an increase of 13% in fracture strength is sufficient (Orwoll et al., 2009). However, it needs to be noted that there is a high range in load-to-strength ratios and many patients are likely not helped with these relatively low strength increases. In the study by Keaveny and Bouxsein, more than 50% of subjects had a load-to-strength ratio over 1.2 and in the study by Orwoll et al., 20% of fracture cases had a load-to-strength ratio above 1.5. This shows that in severely osteoporotic patients hip fractures might not be prevented by injection of the material alone.

This study presents some limitations in the proposed modeling approach. The used mesh density followed from an in-house mesh convergence study and both the material mapping strategy and the failure criterion have been previously validated against ex-vivo experiments (Schileo et al., 2014; Taddei et al., 2007). However, the material properties of the injected material are based on data supplied by the manufacturer. No direct experiments have been conducted on bone with CaS/HA adding uncertainty to the material mapping strategy for the elements within the injection region. This study has also only looked at the primary increase in fracture strength resulting from the injection. Remodeling of the material and the surrounding bone has not yet been taken into account and might be of interest for future investigations. This becomes especially relevant when the potential of the used material to carry bone regenerating agents is taken into account (Raina et al., 2016).

To summarize, we have shown that an injection of a biphasic biomaterial in the proximal femur is clinically feasible but our computational models predict that without proper planning of the injection location, the increase in fracture strength will be limited. By varying the volume, location and stiffness of the injected material one can further increase strength substantially. The highest theoretical increase in fracture strength for a 10 ml injection was found in the lateral part of the femoral neck. This shows that prophylactic injections with CaS/HA have the possibility to provide an immediate reduction in fracture risk.

Acknowledgements

This project has received funding from the Swedish Foundation for Strategic Research (IB2013-0021), Swedish Research Council (2015-04795) and the European Union's Horizon 2020 research and innovation program under the Marie Sklodowska-Curie grant agreement No. 713645. The authors also acknowledge the financial support from VINNOVA, the Swedish agency for innovation systems (grant number 2017-00269).

Conflict of interest disclosure

Lars Lidgren is a board member of Bone Support AB and Orthocell. Other authors have no conflicts of interest.

Appendix A. Supplementary data

Supplementary data to this article can be found online at https://doi.org/10.1016/j.clinbiomech.2019.03.008.

References

Basafa, E., Armand, M., 2014. Subject-specific planning of femoroplasty: a combined evolutionary optimization and particle diffusion model approach. J. Biomech. 47, 2237–2243. https://doi.org/10.1016/j.jbiomech.2014.05.002.

Basafa, E., Murphy, R.J., Otake, Y., Kutzer, M.D., Belkoff, S.M., Mears, S.C., Armand, M., 2015. Subject-specific planning of femoroplasty: an experimental verification study. J. Biomech. 48, 59–64. https://doi.org/10.1016/j.jbiomech.2014.11.002.

Bayraktar, H.H., Morgan, E.F., Niebur, G.L., Morris, G.E., Wong, E.K., Keaveny, T.M., 2004. Comparison of the elastic and yield properties of human femoral trabecular and cortical bone tissue. J. Biomech. 37, 27–35. https://doi.org/10.1016/S0021-9290(03)00257-4.

Beckmann, J., Springorum, R., Vettorazzi, E., Bachmeier, S., Lüring, C., Tingart, M., Püschel, K., Stark, O., Grifka, J., Gehrke, T., Amling, M., Gebauer, M., 2011. Fracture prevention by femoroplasty-cement augmentation of the proximal femur. J. Orthop. Res. 29, 1753–1758. https://doi.org/10.1002/jor.21410.

Berry, S.D., Samelson, E.J., Hannan, M.T., Mclean, R.R., Lu, M., Cupples, L.A., Shaffer, M.L., Beiser, A.L., Kelly-hayes, M., Kiel, D.P., 2008. Second Hip Fracture in Older Men and Women. 167. pp. 1971–1976.

Burge, R., Dawson-Hughes, B., Solomon, D.H., Wong, J.B., King, A., Tosteson, A., 2007. Incidence and economic burden of osteoporosis-related fractures in the United States, 2005–2025. J. Bone Miner. Res. 22, 465–475. https://doi.org/10.1359/jbmr.061113.

Ferrari, S., Reginster, J.-Y., Brandi, M.L., Kanis, J.A., Devogelaer, J.-P., Kaufman, J.-M., Féron, J.-M., Kurth, A., Rizzoli, R., 2016. Unmet needs and current and future approaches for osteoporotic patients at high risk of hip fracture. Arch. Osteoporos. 11, 37. https://doi.org/10.1007/s11657-016-0292-1.

Heini, P.F., Franz, T., Fankhauser, C., Gasser, B., Ganz, R., 2004. Femoroplasty-augmentation of mechanical properties in the osteoporotic proximal femur: a biomechanical investigation of PMMA reinforcement in cadaver bones. Clin. Biomech. 19, 506–512. https://doi.org/10.1016/j.clinbiomech.2004.01.014.

Hernlund, E., Svedbom, A., Ivergård, M., Compston, J., Cooper, C., Stenmark, J., McCloskey, E.V., Jönsson, B., Kanis, J.A., 2013. Osteoporosis in the European Union: medical management, epidemiology and economic burden: a report prepared in collaboration with the International Osteoporosis Foundation (IOF) and the European Federation of Pharmaceutical Industry Associations (EFPIA). Arch. Osteoporos. 8. https://doi.org/10.1007/s11657-013-0136-1.

Järvinen, T.L.N., Michaëlsson, K., Jokihaara, J., Collins, G.S., Perry, T.L., Mintzes, B., Musini, V., Erviti, J., Gorricho, J., Wright, J.M., Sievänen, H., 2015. Overdiagnosis of bone fragility in the quest to prevent hip fracture. BMJ 350, h2088. https://doi.org/10.1136/bmj.h2088.

Keaveny, T.M., Bouxsein, M.L., 2008. Theoretical implications of the biomechanical fracture threshold. J. Bone Miner. Res. 23, 1541–1547. https://doi.org/10.1359/jbmr.080406.

Kinzl, M., Boger, A., Zysset, P.K., Pahr, D.H., 2011. The effects of bone and pore volume fraction on the mechanical properties of PMMA/bone biopsies extracted from augmented vertebrae. J. Biomech. 44, 2732–2736. https://doi.org/10.1016/j.jbiomech.2011.07.028.

Masala, S., Nano, G., Marcia, S., Muto, M., Fucci, F.P.M., Simonetti, G., 2012. Osteoporotic vertebral compression fractures augmentation by injectable partly resorbable ceramic bone substitute (Cerament™|SPINE SUPPORT): a prospective non-randomized study. Neuroradiology 54, 589–596. https://doi.org/10.1007/s00234-011-0940-5.

Morgan, E.F., Bayraktar, H.H., Keaveny, T.M., 2003. Trabecular bone modulus-density relationships depend on anatomic site. J. Biomech. 36, 897–904. https://doi.org/10.1016/S0021-9290(03)00071-X.

Nilsson, M., Zheng, M.H., Tägil, M., 2013. The composite of hydroxyapatite and calcium sulphate: a review of preclinical evaluation and clinical applications. Expert Rev. Med. Devices. https://doi.org/10.1586/17434440.2013.827529.

Orwoll, E.S., Marshall, L.M., Nielson, C.M., Cummings, S.R., Lapidus, J., Cauley, J.A., Ensrud, K., Lane, N., Hoffmann, P.R., Kopperdahl, D.L., Keaveny, T.M., 2009. Finite element analysis of the proximal femur and hip fracture risk in older men. J. Bone Miner. Res. 24, 475–483. https://doi.org/10.1359/jbmr.081201.

Raina, D.B., Isaksson, H., Hettwer, W., Kumar, A., Lidgren, L., Tägil, M., 2016. A biphasic calcium sulphate/hydroxyapatite carrier containing bone morphogenic protein-2 and zoledronic acid generates bone. Nat. Publ. Group 1–13. https://doi.org/10.1038/srep26033.

Saita, Y., Ishijima, M., Kaneko, K., 2015. Atypical femoral fractures and bisphosphonate use: current evidence and clinical implications 185–193. doi:https://doi.org/10.1177/2040622315584114.

Santesso, N., Carrasco-Labra, A., Brignardello-Petersen, R., 2014. Hip protectors for preventing hip fractures in older people. Cochrane Database Syst. Rev. https://doi.org/10.1002/14651858.CD001255.pub5.

Schileo, E., Balistreri, L., Grassi, L., Cristofolini, L., Taddei, F., 2014. To what extent can linear finite element models of human femora predict failure under stance and fall loading configurations? J. Biomech. 47, 3531–3538. https://doi.org/10.1016/j.jbiomech.2014.08.024.

Sobolev, B., Sheehan, K.J., Kuramoto, L., Guy, P., 2015. Risk of second hip fracture persists for years after initial trauma. Bone 75, 72–76. https://doi.org/10.1016/j.bone.2015.02.003.

Taddei, F., Schileo, E., Helgason, B., Cristofolini, L., Viceconti, M., 2007. The material mapping strategy influences the accuracy of CT-based finite element models of bones: an evaluation against experimental measurements. Med. Eng. Phys. 29, 973–979. https://doi.org/10.1016/j.medengphy.2006.10.014.

Varga, P., Hofmann-Fliri, L., Blauth, M., Windolf, M., 2016. Prophylactic augmentation of the osteoporotic proximal femur—mission impossible? Bonekey Rep. 5, 7270. https://doi.org/10.1038/bonekey.2016.86.

Varga, P., Inzana, J.A., Schwiedrzik, J., Zysset, P.K., Gueorguiev, B., Blauth, M., Windolf, M., 2017. New approaches for cement-based prophylactic augmentation of the osteoporotic proximal femur provide enhanced reinforcement as predicted by non-linear finite element simulations. Clin. Biomech. 44, 7–13. https://doi.org/10.1016/j.clinbiomech.2017.03.001.

Warriner, A.H., Patkar, N.M., Curtis, J.R., Delzell, E., Gary, L., Kilgore, M., Saag, K., 2011. Which fractures are most attributable to osteoporosis? J. Clin. Epidemiol. 64, 46–53. https://doi.org/10.1016/j.jclinepi.2010.07.007.